Bottomonium Observables in Heavy-Ion Collisions Using Open Quantum Systems and Effective Field Theories

Rencontre Ions Lourds

Peter Vander Griend

University of Kentucky
Fermi National Accelerator Laboratory

24 November 2022

Introduction

Motivation: use heavy quarks and their bound states to probe the strongly coupled medium formed in heavy ion collisions

- high mass M of bottom quarks and the short formation time of their bound states make them ideal probes of the quark gluon plasma (QGP); observables of interest include nuclear suppression factor R_{AA} and elliptic flow v_2
- ideally suited for treatment using the formalism of open quantum systems (OQS) and effective field theory (EFT)
  - OQS: allows for the rigorous treatment of a quantum system of interest (heavy quarkonium) coupled to and evolving out of equilibrium with an environment (QGP)
  - EFTs: take advantage of the large mass of the heavy quark and the resulting nonrelativistic nature of the system and small bound state radius using potential nonrelativistic QCD (pNRQCD), an EFT of the strong interaction

Advantages: fully quantum, non-Abelian, heavy quark number conserving, account for dissociation and recombination, and valid for strong or weak coupling

Background

Heavy Quarkonium Suppression

- quark and antiquark bound by confining potential

$$V(r) \sim -\frac{4}{3}\frac{\alpha_s}{r} + \sigma r$$

- in medium, potential gluons are Debye screened
- for $r_{q\bar{q}} \gtrsim r_D$, state dissociates due to screening and fewer $q\bar{q}$ states are observed compared to naive expectation from pp collisions
- suppression of the J/ψ theorized to signal the formation of a a deconfined QGP[1]

[1] Phys. Lett. B 178 (1986) 416-422 (Matsui and Satz)

Heavy Quarkonium Suppression: Modern Perspective

Heavy Quarkonium Suppression

- paradigmatic shift in understanding of heavy quarkonium suppression with the finding of a nonzero imaginary part of in-medium potential[2,3]
- imaginary part of potential related to in-medium width and decay; large in screening regime
- recombination a significant effect in the charm sector, and the J/ψ less suppressed than naively expected

[2] JHEP 03 (2007) 054 (Laine, Philipsen, Romatschke, Tassler)
[3] Phys. Rev. D 78 (2008) 014017 (Brambilla, Ghiglieri, Petreczky, Vairo)

Physical Setup

relevant energy scales (EFT)

- heavy quark mass $M = M_b \sim 5$ GeV
- inverse Bohr radius $1/a_0 \sim 1.5$ GeV
- (π times) the temperature of the medium $(\pi)T \sim 1.5$ GeV
- (Coulombic) binding energy $E \sim 0.5$ GeV
- hierarchical ordering: $M \gg 1/a_0 \gg (\pi)T \gg E$ [4]

relevant time scales (OQS)

- system intrinsic time scale: $\tau_S \sim 1/E$
- environment correlation time: $\tau_E \sim 1/(\pi T)$
- relaxation time: $\tau_R \sim 1/\Sigma_s \sim 1/(a_0^2(\pi T)^3)$ (where Σ_s is the thermal self energy)

---

[4] $\pi T \sim 1.5$ GeV at initial time; medium quickly expands and cools such that $1/a_0 \gg \pi T$ is realized

Hierarchies and Simplifying Assumptions

quantum Brownian motion

for

$$\tau_R, \tau_S \gg \tau_E,$$

where τ_R, τ_S, and τ_E are the relaxation, system intrinsic, and environment correlation time scales, respectively, the system realizes **quantum Brownian motion**

Simplifying Approximations

hierarchy of scales allows for two simplifying approximations:

- **Born approximation**: quarkonium has little effect on the medium at time scales of interest; density matrix factorizes, i.e., $\rho(t) \propto \rho_S(t) \otimes \rho_E$
- **Markov approximation**: only the state of the quarkonium at the present time is necessary to describe its evolution, i.e., no memory integral

potential Non-Relativistic QCD (pNRQCD)

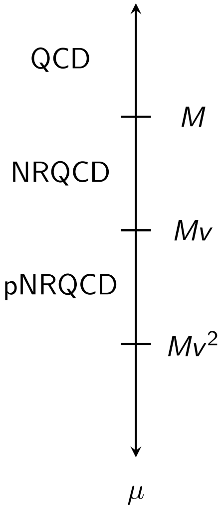

- effective theory of the strong interaction obtained from full QCD via non-relativistic QCD (NRQCD) by successive integrating out of the hard (M) and soft (Mv) scales where $v \ll 1$ is the relative velocity in a heavy-heavy bound state
- degrees of freedom are singlet and octet heavy-heavy bound states and ultrasoft gluons
- small bound state radius and large quark mass allow for double expansion in r and M^{-1} at the Lagrangian level

pNRQCD Lagrangian[5]

$$\mathcal{L}_{\text{pNRQCD}} = \text{Tr}\Big[S^\dagger(i\partial_0 - h_s)S + O^\dagger(iD_0 - h_o)O + O^\dagger \mathrm{r}\cdot g\,\mathrm{E}\,S$$
$$+S^\dagger \mathrm{r}\cdot g\,\mathrm{E}\,O + \frac{1}{2}O^\dagger\,\{\mathbf{r}\cdot g\,\mathrm{E}\,,\,O\}\Big]$$

- singlet and octet field S and O interacting via chromo-electric dipole vertices
- $h_{s,o} = \frac{\mathrm{p}^2}{M} + V_{s,o}$: singlet, octet Hamiltonian
  - $V_s = -\frac{C_f\alpha_s(1/a0)}{r}$: attractive singlet potential
  - $V_o = \frac{\alpha_s(1/a0)}{2N_c r}$: repulsive octet potential
- $iD_0 O = i\partial_0 O - [gA_0, O]$
  - commutator can be eliminated via field redefinition

$$E^{a,i}(s,\mathbf{0}) \to \tilde{E}^{a,i}(s,\mathbf{0}) = \Omega(s)E^{a,i}(s,\mathbf{0})\Omega(s)^\dagger$$

where

$$\Omega(s) = \exp\left[-ig\int_{-\infty}^{s}\mathrm{d}s'A_0(s',\mathbf{0})\right]$$

[5] Nucl.Phys.B 566 (2000) 275; Rev.Mod.Phys. 77 (2005) 1423 (Brambilla, Pineda, Soto, Vairo)

Evolution Equations[6]

evolution equations of in-medium Coulombic heavy quarkonium given by:

$$
\begin{aligned}
\frac{\mathrm{d}\rho_s(t)}{\mathrm{d}t} &= -\, i\,[h_s, \rho_s(t)] - \Sigma_s \rho_s(t) - \rho_s(t)\Sigma_s^\dagger + \Xi_{so}(\rho_o(t)) \\
\frac{\mathrm{d}\rho_o(t)}{\mathrm{d}t} &= -\, i\,[h_o, \rho_o(t)] - \Sigma_o \rho_o(t) - \rho_o(t)\Sigma_o^\dagger + \Xi_{os}(\rho_s(t)) \\
&\quad + \Xi_{oo}(\rho_o(t))
\end{aligned}
$$

where the Σ and Ξ encode interactions with the medium and can be computed diagrammatically in pNRQCD

[6] Phys. Rev. D 97 (2018) 7, 074009 (Brambilla, Escobedo, Soto, Vairo)

Diagrammatic Evolution of $\rho_s(t)$

singlet evolution given by

$$\frac{\mathrm{d}\rho_s(t)}{\mathrm{d}t} = -i\,[h_s, \rho_s(t)] - \Sigma_s \rho_s(t) - \rho_s(t)\Sigma_s^\dagger + \Xi_{so}(\rho_o(t))$$

where

$\Sigma_s \rho_s(t) \sim$ 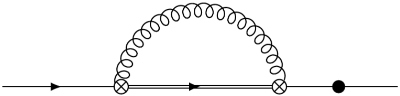

$\Xi_{so}(\rho_o(t)) \sim$ 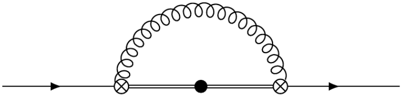

Diagramatic Evolution of $\rho_o(t)$

octet evolution given by

$$\frac{\mathrm{d}\rho_o(t)}{\mathrm{d}t} = -i\,[h_o, \rho_o(t)] - \Sigma_o \rho_o(t) - \rho_o(t)\Sigma_o^\dagger + \Xi_{os}(\rho_s(t)) + \Xi_{oo}(\rho_o(t))$$

where

$\Sigma_o \rho_o(t) \sim$ 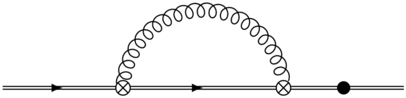

$\Xi_{os}(\rho_s(t)) \sim$ 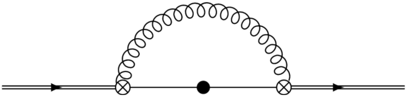

$\Xi_{oo}(\rho_o(t)) \sim$ 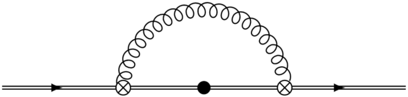

Master Equation

evolution equations can be rewritten as master equation

$$\frac{\mathrm{d}\rho(t)}{\mathrm{d}t} = -i[H, \rho(t)] + \sum_{n,m} h_{nm} \left(L_i^n \rho(t) L_i^{m\dagger} - \frac{1}{2} \left\{ L_i^{m\dagger} L_i^n, \rho(t) \right\} \right),$$

where

$$\rho(t) = \begin{pmatrix} \rho_s(t) & 0 \\ 0 & \rho_o(t) \end{pmatrix}, \quad H = \begin{pmatrix} h_s + \mathrm{Im}(\Sigma_s) & 0 \\ 0 & h_o + \mathrm{Im}(\Sigma_o) \end{pmatrix},$$

$$L_i^0 = \begin{pmatrix} 0 & 0 \\ 0 & 1 \end{pmatrix} r^i, \quad L_i^1 = \begin{pmatrix} 0 & 0 \\ 0 & \frac{N_c^2-4}{2(N_c^2-1)} A_i^{oo\dagger} \end{pmatrix}, \quad L_i^2 = \begin{pmatrix} 0 & \frac{1}{\sqrt{N_c^2-1}} \\ 1 & 0 \end{pmatrix} r^i,$$

$$L_i^3 = \begin{pmatrix} 0 & \frac{1}{\sqrt{N_c^2-1}} A_i^{os\dagger} \\ A_i^{so\dagger} & 0 \end{pmatrix}, \quad h = \begin{pmatrix} 0 & 1 & 0 & 0 \\ 1 & 0 & 0 & 0 \\ 0 & 0 & 0 & 1 \\ 0 & 0 & 1 & 0 \end{pmatrix},$$

$$\boxed{A_i^{uv} = \frac{g^2}{6N_c} \int_0^\infty \mathrm{d}s \, e^{-ih_u s} r^i e^{ih_v s} \langle \tilde{E}^{a,j}(0, \mathbf{0}) \tilde{E}^{a,j}(s, \mathbf{0}) \rangle}$$

Lindblad Equation

- for $(\pi)T \gtrsim E$, $e^{-ih_{s,o}s} \approx 1 - ih_{s,o}s$ and medium interactions simplify

$$A_i^{uv} = \frac{r_i}{2}(\kappa - i\gamma) + \kappa\left(-\frac{ip_i}{2MT} + \frac{\Delta V_{uv}}{4T} r_i\right),$$

where

$$\kappa = \frac{g^2}{6N_c}\int_0^\infty \mathrm{d}t \left\langle \left\{ \tilde{E}_i^a(t,0), \tilde{E}_i^a(0,0) \right\} \right\rangle,$$

$$\gamma = -\frac{ig^2}{6N_c}\int_0^\infty \mathrm{d}t \left\langle \left[\tilde{E}_i^a(t,0), \tilde{E}_i^a(0,0) \right] \right\rangle,$$

$$\frac{\kappa}{4T} = \frac{ig^2}{6N_c}\int_0^\infty \mathrm{d}t\, t \left\langle \tilde{E}_i^a(t,0)\tilde{E}_i^a(0,0) \right\rangle$$

- κ is the momentum diffusion coefficient occurring in a Langevin equation describing the diffusion of a heavy particle[7]; γ is its dispersive counterpart

[7] Phys. Rev. D 74 (2006) 085012 (Casalderrey-Solana, Teaney)

Lindblad Equation at order $(E/T)^0$

at order 0 in the E/T expansion, evolution equations can be brought into form of a Lindblad equation

$$\frac{\mathrm{d}\rho(t)}{\mathrm{d}t} = -i[H, \rho(t)] + \sum_n \left(C_i^n \rho(t) C_i^{n\dagger} - \frac{1}{2} \left\{ C_i^{n\dagger} C_i^n, \rho(t) \right\} \right)$$

where H is the quarkonium Hamiltonian, and the C^n are collapse operators resulting from interactions with the medium

$$\rho = \begin{pmatrix} \rho_s & 0 \\ 0 & \rho_o \end{pmatrix}, \quad H = \begin{pmatrix} h_s & 0 \\ 0 & h_o \end{pmatrix} + \frac{r^2}{2}\gamma \begin{pmatrix} 1 & 0 \\ 0 & \frac{N_c^2-2}{2(N_c^2-1)} \end{pmatrix},$$

$$C_i^0 = \sqrt{\frac{\kappa}{N_c^2-1}} r_i \begin{pmatrix} 0 & 1 \\ \sqrt{N_c^2-1)} & 0 \end{pmatrix}, \quad C_i^1 = \sqrt{\frac{(N_c^2-4)\kappa}{2(N_c^2-1)}} r_i \begin{pmatrix} 0 & 0 \\ 0 & 1 \end{pmatrix}$$

medium interactions specified by κ and γ

Lindblad Equation at order $(E/T)^2$

at order E/T, master equation cannot be written as Lindblad equation; however, we can write a Lindblad equation containing terms up to and including order $(E/T)^2$ equivalent to order (E/T) master equation

$$H = \begin{pmatrix} h_s & 0 \\ 0 & h_o \end{pmatrix} + \left(\frac{r^2}{2}\gamma + \frac{\kappa}{4MT}\{r_i, p_i\} \right) \begin{pmatrix} 1 & 0 \\ 0 & \frac{N_c^2-2}{2(N_c^2-1)} \end{pmatrix},$$

$$C_i^0 = \sqrt{\frac{\kappa}{N_c^2-1}} \left(r^i + \frac{ip_i}{2MT} + \frac{\Delta V_{os}}{4T} r_i \right) \begin{pmatrix} 0 & 1 \\ 0 & 0 \end{pmatrix}$$

$$+ \sqrt{\kappa} \left(r_i + \frac{ip_i}{2MT} + \frac{\Delta V_{os}}{4T} r_i \right) \begin{pmatrix} 0 & 0 \\ 1 & 0 \end{pmatrix},$$

$$C_i^1 = \sqrt{\frac{(N_c^2-4)\kappa}{2(N_c^2-1)}} \left(r_i + \frac{ip_i}{2MT} \right) \begin{pmatrix} 0 & 0 \\ 0 & 1 \end{pmatrix}$$

medium interactions still specified by κ and γ

Transport Coefficients

- κ is the heavy quarkonium momentum diffusion coefficient; γ is its dispersive counterpart
- κ and γ related to in-medium width and mass shift of $\Upsilon(1S)$:

$$\Gamma(1S) = 3a_0^2\kappa, \quad \delta M(1S) = \frac{3}{2}a_0^2\gamma,$$

  and accessible from unquenched lattice measurements of Γ and δM
- temperature dependent heavy quark momentum diffusion coefficient can be extracted from chromo-electric correlation functions measurable on the lattice

Extraction of κ

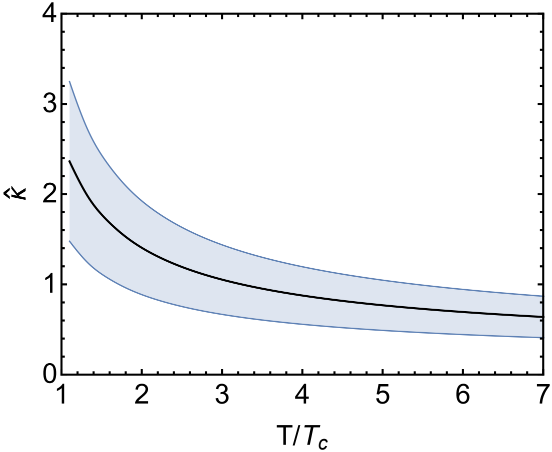

Figure: Direct, quenched lattice measurement of $\hat{\kappa} = \kappa/T^3$.[8]

We solve the Lindlbad equation using the upper, central, and lower $\hat{\kappa}(T) = \kappa(T)/T^3$ curves.

[8] Phys. Rev. D 102, 074503 (2020) (Brambilla, Leino, Petreczky, Vairo)

Extraction of γ

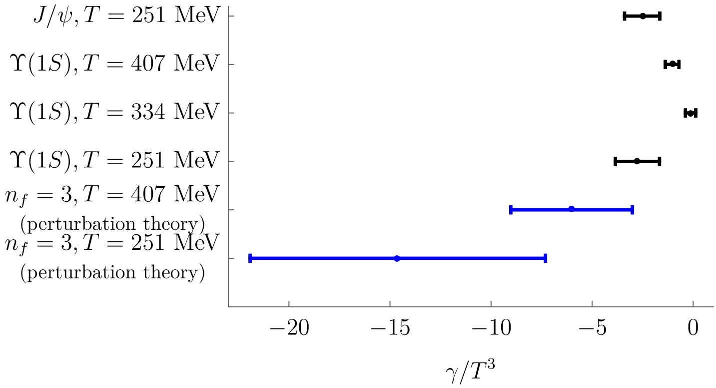

Figure: Indirect extractions[9] of $\hat{\gamma} = \gamma/T^3$ from unquenched lattice measurements of $\delta M(1S)$.[10]

We solve the Lindlbad equation in the range $-3.5 \leq \gamma/T^3 \leq 0$.

[9] adapted from Phys. Rev. D 100 (2019) 5, 054025 (Brambilla, Escobedo, Vairo, PVG)

[10] JHEP 11 (2018) 088 (Kim, Petreczky, Rothkopf); Phys.Rev.D 100 (2019) 7, 074506 (Larsen, Meinel, Mukherjee, Petreczky).

Quantum Trajectories Algorithm

- Monte Carlo method to solve the Lindblad equation
- less memory intensive due to use of wave function $|\psi\rangle$ rather than density matrix ρ
- absorb quantum number conserving diagonal evolution terms of Lindblad equation into a non-Hermitian effective Hamiltonian

$$H_{eff} = H - \frac{i}{2}\sum_n C_n^\dagger C_n$$

  Lindblad equation becomes

$$\frac{\mathrm{d}\rho(t)}{\mathrm{d}t} = -i\left(H_{eff}\,\rho(t) - \rho(t)H_{eff}^\dagger\right) + \sum_n C_i^n \rho(t) C_i^{n\dagger}$$

- H_{eff} term reduces trace of ρ and preserves quantum numbers of state
- C_n term changes quantum numbers of state and ensure overall evolution is trace preserving

H_{eff} Evolution

- evolve wavefunction with H_{eff}

$$|\psi(t+\delta t)\rangle = (1 - iH_{eff}\delta t)|\psi(t)\rangle$$

- H_{eff} evolution preserves quantum numbers of the state and decreases its norm

$$\begin{aligned}\langle\psi(t+\delta t)|\psi(t+\delta t)\rangle &\approx 1 - i\langle\psi(t)|(H_{eff} - H_{eff}^{\dagger})|\psi(t)\rangle\delta t \\ &= 1 - \delta p\end{aligned}$$

where

$$\delta p = \sum_n \langle\psi(t)|C_n^{\dagger}C_n|\psi(t)\rangle\delta t = \sum_n \delta p_n$$

- decrease in norm related to probability a change of quantum numbers, implemented by $C_n|\psi(t)\rangle$, occurs

Monte Carlo

(normalized) evolution of state

$$|\tilde{\psi}(t+\delta t)\rangle = \begin{cases} \frac{|\psi(t+\delta t)\rangle}{\sqrt{1-\delta p}} & \text{with probability } 1-\delta p \\ \frac{C_n|\psi(t)\rangle}{\sqrt{\delta p_n/\delta t}} & \text{with probability } \delta p \end{cases}$$

i.e., with probability $1-\delta p$, the state evolves as governed by H_{eff}, and with probability δp, is acted on by the collapse operator C_n

simulation

- generate a random number $0 < r_1 < 1$
- evolve state with H_{eff} until norm squared $< r_1$
- generate additional random number(s) to determine which collapse operator C_n to apply

Equivalence of Evolution and Convergence

equivalence of evolution

$$
\begin{aligned}
\rho(t+\delta t) =& (1-\delta p)\frac{|\psi(t+\delta t)\rangle}{\sqrt{1-\delta p}}\frac{\langle\psi(t+\delta t)|}{\sqrt{1-\delta p}} \\
&+ \delta p \sum_n \frac{\delta p_n}{\delta p}\frac{C_n|\psi(t)\rangle}{\sqrt{\delta p_n/\delta t}}\frac{\langle\psi(t)|C_n^\dagger}{\sqrt{\delta p_n/\delta t}} \\
=& \rho(t) - i[H_{eff}\rho(t) - \rho(t)H_{eff}^\dagger]\delta t + \sum_n C_n\rho(t)C_n^\dagger\delta t,
\end{aligned}
$$

as given by Lindblad equation

convergence

- calculate expectation values using evolved state
- evolve many states and average to converge to result of directly solving the Lindblad equation

QTraj Implementation[11]

1. initialize wave function $|\psi(t_0)\rangle$
2. generate random number $0 < r_1 < 1$, evolve with $H_{\rm eff}$ until

$$|| \, e^{-i\int_{t_0}^{t} dt' H_{\rm eff}(t')} |\psi(t_0)\rangle \, ||^2 \leq r_1,$$

   and initiate a quantum jump
3. quantum jump
   - 3.1 if singlet, jump to octet; if octet, generate random number $0 < r_2 < 1$ and jump to singlet if r_2 less than the branching fraction to singlet; otherwise, remain in octet
   - 3.2 generate random number $0 < r_3 < 1$; if $r_3 < l/(2l+1)$, $l \to l-1$; otherwise, $l \to l+1$.
   - 3.3 multiply wavefunction by r and normalize
4. Continue from step 2.

[11] Comput. Phys. Commun. 273 (2022) 108266 (Ba Omar, et. al.)

Code Output to Experimental Observables

- each realization of the `QTraj` algorithm is a *quantum trajectory*
- average of N quantum trajectories tends toward the solution of the Lindblad equation as $N \to \infty$
- overlap of resulting average trajectory with eigenstates, e.g., $\Upsilon(1S)$, $\Upsilon(2S)$, etc., used to compute survival probability of that state
- after accounting for feed down of excited states, results can be compared to experiment

Medium Interaction

- medium evolution implemented using a $3 + 1$D dissipative relativistic hydrodynamics code using a realistic equation of state fit to lattice QCD measurements
- approximately $7 - 9 \times 10^5$ physical trajectories
  - production point sampled in transverse plane using nuclear binary collision overlap profile $N_{AA}^{\rm bin}(x, y, b)$, initial p_T from an E_T^{-4} spectrum, and ϕ uniformly in $[0, 2\pi)$
  - 50-100 quantum trajectories per physical trajectory
  - allows for extraction of differential obserables including v_2 and results as a function of transverse momentum p_T
- vacuum evolution from initialization at $t_0 = 0$ fm until initialization of interaction with medium at $t = 0.6$ fm and vacuum evolution for $T < T_f = 190$ MeV (NLO E/T) and $T < T_f = 250$ MeV (LO E/T)

R_{AA} vs. Centrality

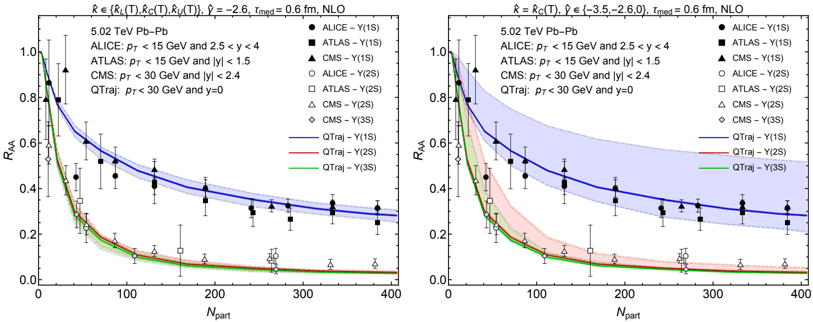

Figure: R_{AA} for the $\Upsilon(1S)$, $\Upsilon(2S)$, and $\Upsilon(3S)$ as a function of centrality compared to experimental measurements. The left panel shows variation of $\hat{\kappa} \in \{\kappa_L(T), \kappa_C(T), \kappa_U(T)\}$ and the right panel shows variation of $\hat{\gamma}$ in the range $-3.5 \leq \hat{\gamma} \leq 0$. In both panels, the solid line corresponds to $\hat{\kappa} = \hat{\kappa}_C(T)$ and the best fit value of $\hat{\gamma} = -2.6$. NLO in E/T.[12]

[12] JHEP 08 (2022) 303 (Brambilla, Escobedo, Islam, Strickland, Tiwari, Vairo, PVG)

R_{AA} vs. p_T

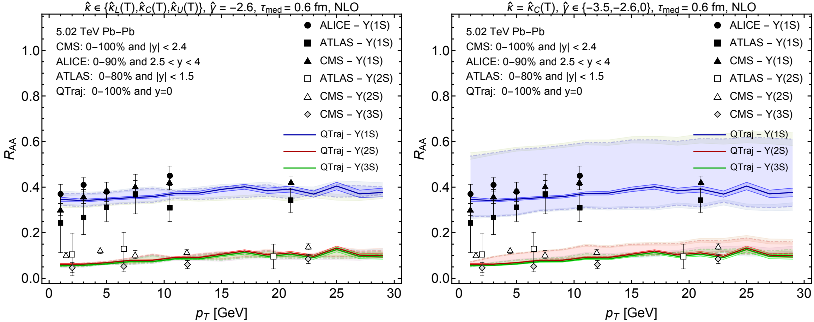

Figure: R_{AA} for the $\Upsilon(1S)$, $\Upsilon(2S)$, and $\Upsilon(3S)$ as a function of p_T compared to experimental measurements. NLO in E/T.[13]

[13] JHEP 08 (2022) 303 (Brambilla, Escobedo, Islam, Strickland, Tiwari, Vairo, PVG)

Double Ratio 2S vs. Centrality

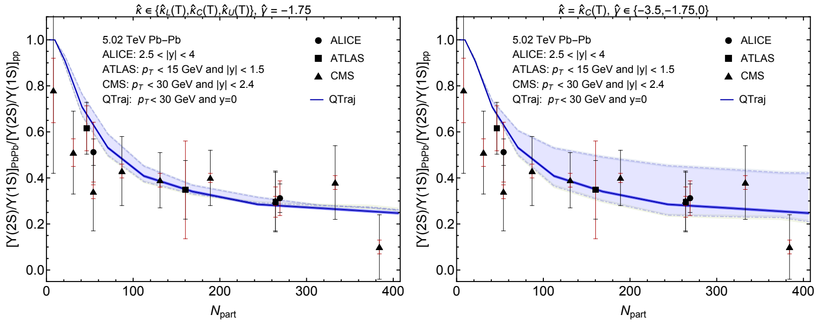

Figure: Double ratio of $R_{AA}(2S)$ to $R_{AA}(1S)$ as a function of centrality compared to experimental measurements. The left panel shows variation of $\hat{\kappa} \in \{\kappa_L(T), \kappa_C(T), \kappa_U(T)\}$ and the right panel shows variation of $\hat{\gamma}$ in the range $-3.5 \le \hat{\gamma} \le 0$. In both panels, the solid line corresponds to $\hat{\kappa} = \hat{\kappa}_C(T)$ and the best fit value of $\hat{\gamma} = -1.75$. LO in E/T.[14]

---

[14] Phys. Rev. D 104 (2021) 9, 094049 (Brambilla, Escobedo, Strickland, Vairo, PVG, Weber)

Double Ratio $3S$ vs. Centrality

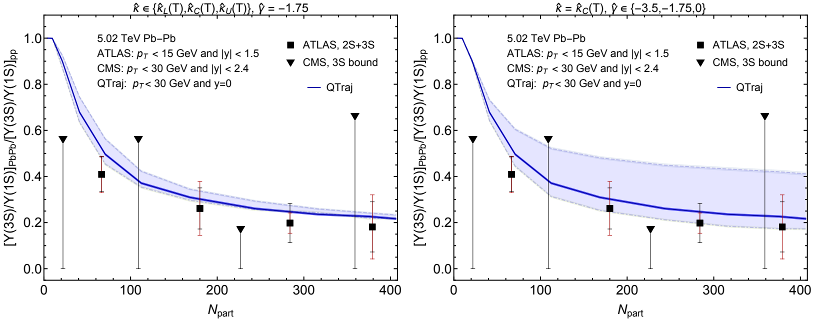

Figure: Double ratio of $R_{AA}(3S)$ to $R_{AA}(1S)$ as a function of centrality compared to experimental measurements. LO in E/T.[15]

[15] Phys. Rev. D 104 (2021) 9, 094049 (Brambilla, Escobedo, Strickland, Vairo, PVG, Weber)

Double Ratio $2S$ vs. p_T

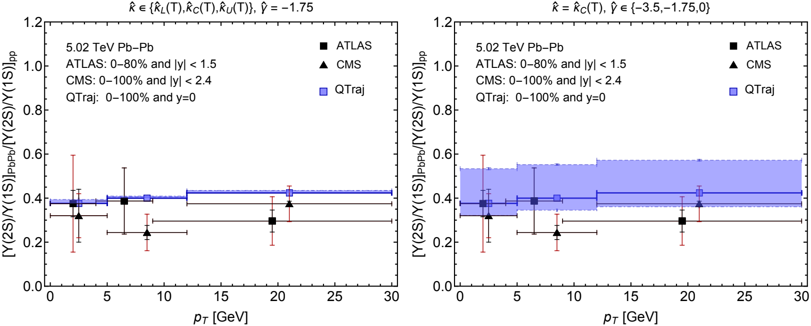

Figure: Double ratio of $R_{AA}(2S)$ to $R_{AA}(1S)$ as a function of p_T compared to experimental measurements. LO in E/T.[16]

[16] Phys. Rev. D 104 (2021) 9, 094049 (Brambilla, Escobedo, Strickland, Vairo, PVG, Weber)

$v_2[\Upsilon(1S)]$ vs. Centrality

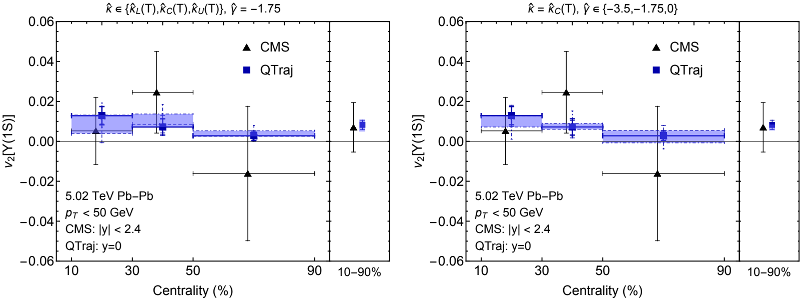

Figure: The elliptic flow v_2 of the $\Upsilon(1S)$ as a function of centrality compared to experimental measurements. LO in E/T.[17]

[17] Phys. Rev. D 104 (2021) 9, 094049 (Brambilla, Escobedo, Strickland, Vairo, PVG, Weber)

$v_2[\Upsilon(1S)]$ vs. p_T

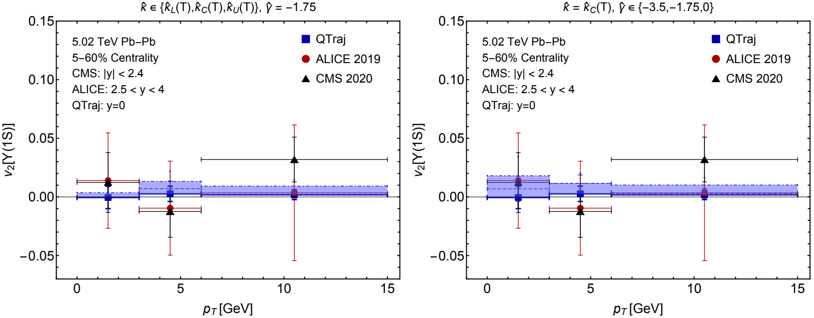

Figure: The elliptic flow v_2 of the $\Upsilon(1S)$ as a function of p_T compared to experimental measurements. LO in E/T.[18]

[18] Phys. Rev. D 104 (2021) 9, 094049 (Brambilla, Escobedo, Strickland, Vairo, PVG, Weber)

$v_2[\Upsilon(2,3S)]$ vs. Centrality

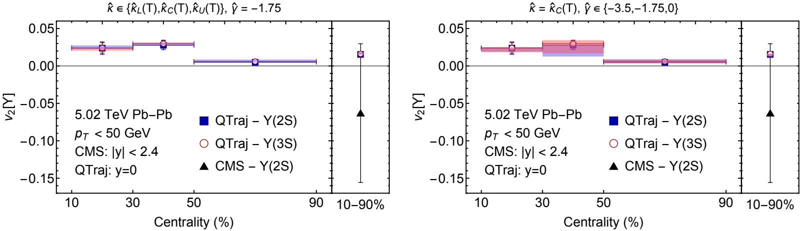

Figure: The elliptic flow v_2 of the $\Upsilon(2S)$ and $\Upsilon(3S)$ as a function of centrality compared to experimental measurements. LO in E/T.[19]

[19] Phys. Rev. D 104 (2021) 9, 094049 (Brambilla, Escobedo, Strickland, Vairo, PVG, Weber)

Experimental References

Plot	Reference (Experiment)
R_{AA} and double ratios	Phys. Lett. B 822 (2021) 136579 (ALICE) link to presentation (ATLAS) Phys. Rev. Lett 120 142301 (2018) (CMS) Phys. Lett. B 790 (2019) 270 (CMS) link to presentation (CMS)
v_2	Phys. Rev. Lett. 123, 192301 (2019) (ATLAS) Phys. Lett. B 819 (2021) 136385 (CMS)

Conclusions and Outlook

- due to hierarchies of scale, system of in-medium bottomonium ideally described using EFT methods, specifically pNRQCD, and the OQS formalism
- evolution equation takes the form of a Lindblad equation
- computational methods necessary to solve the Lindblad equation and extract observables including R_{AA} and v_2
- `QTraj` code implements the quantum trajectories algorithm to solve the Lindblad equation and extract R_{AA} and v_2 as functions of N_{part} and p_T
- results show good agreement with experimental data
- method and results are fully quantum, non abelian and heavy quark number conserving; take into account dissociation and recombination; quantum field theoretically describe the nonequilibrium evolution and depend only on the transport coefficients κ and γ the values of which we take from lattice data

Thank you!